

# THE THERMAL SUNYAEV-ZEL'DOVICH SIGNATURE OF BARYONS IN THE LOCAL UNIVERSE

CARLOS HERNÁNDEZ-MONTEAGUDO,<sup>1</sup> HY TRAC,<sup>2</sup> RAUL JIMENEZ,<sup>1</sup> LICIA VERDE<sup>1</sup>

*Draft version July 30, 2018*

## ABSTRACT

Using cosmological hydrodynamical simulations, we investigate the prospects of the thermal Sunyaev-Zel'dovich (tSZ) effect to detect the missing baryons in the local universe. We find that at least 80% of the tSZ luminosity is generated in collapsed structures, and that  $\sim 70\%$  of the remaining diffuse tSZ luminosity (i.e.,  $\sim 15\%$  of the total) comes from overdense regions with  $\delta_{gas} > 10$ , such as filaments and superclusters. The gas present in slightly overdense and underdense regions with  $\delta_{gas} < 10$ , despite making up 50% of the total baryon budget, leaves very little tSZ signature: it gives rise to only  $\sim 5\%$  of the total tSZ luminosity. Thus, future Cosmic Microwave Background (CMB) observations will be sensitive to, at best, one half of the missing baryons, improving the current observational status, but still leaving one half unobserved. Since most of the tSZ is generated in haloes, we find a tight correlation between gas pressure and galaxy number density. This allows us to predict the CMB Comptonization from existing galaxy surveys and to forecast the tSZ effect from the local structures probed by the Two Micron All Sky Survey (2MASS) galaxy catalog.

*Subject headings:* cosmology: cosmic microwave background, observations - methods: numerical - galaxies: clusters: general

## 1. INTRODUCTION

Recent cosmological observations like galaxy surveys (e.g., 2dFGRS, Cole et al. (2005), SDSS, Tegmark et al. (2004)), Supernovae (e.g., SNLS, Astier et al. (2006)) or Cosmic Microwave Background (CMB) (e.g., WMAP, Spergel et al. (2003, 2006)) give strong support to the  $\Lambda$ CDM model of the universe, in which only  $\sim 18\%$  of matter is in the form of baryons. Baryons are mostly probed by CMB, Lyman- $\alpha$  forest (e.g., Croft et al. (1998); McDonald et al. (2005)), and X-rays observations. The first two probes show that the Universe, at much younger epochs, contained an amount of baryons that exceeds by a factor of  $\sim 9$  the baryons seen in today's universe, (Fukugita & Peebles 2004). This is the missing baryons problem. Indeed, according to Cen & Ostriker (1999, 2005), about half of the baryons should be in the form of a Warm Hot Intergalactic Medium (WHIM), at relatively high temperature ( $\sim 10^5 - 10^7$  K) but low densities. Only a small fraction of the total gas is hot enough ( $\gtrsim 10^8$  K) to enable X-ray detection via *bremmstrahlung*: this mechanism led in the nineties to the identification of massive galaxy clusters from ROSAT X-ray observations (e.g., Böhringer et al. (2000)), and more recently has motivated the search (and tentative detections) of diffuse X-ray emission from filaments and superclusters, (Kull & Böhringer 1999; Zappacosta et al. 2002). Although further pieces of evidence for local gas have been found in quasar spectra, in the form of Oxygen absorption features at  $z \simeq 0$  (Nicastro et al. 2005a,b), it is clear that we do not have a complete map of the baryon distribution in the local Universe.

With the advent of high resolution and high sensi-

tivity CMB experiments it has been proposed to trace the local gas using the thermal Sunyaev-Zel'dovich effect (tSZ, Sunyaev & Zeldovich (1980)). The tSZ effect describes the Compton scattering of CMB photons off hot electrons, in which a net transfer of energy from electrons to radiation distorts the Black Body spectrum of the CMB. The relative intensity fluctuations introduced in this scattering are redshift independent, and their amplitude is proportional to the integrated electron pressure along the line of sight. Observational efforts by Génova-Santos et al. (2005) and Battistelli et al. (2006) have detected strong decrements in Corona Borealis, and interpreted them as Compton scattering being generated by extended gas in a filament aligned with the line of sight. Other studies (Hansen et al. 2005; Dolag et al. 2005; Atrio-Barandela & Mücke 2006) addressed this problem from a theoretical point of view, trying to characterize the tSZ signal generated by non-collapsed baryons.

Here we use a hydrodynamical numerical simulation to explore the prospects of future tSZ observations to search for the missing baryons. We find that, as the tSZ effect is sensitive to gas pressure, most of the tSZ luminosity (around 80%) is generated in collapsed structures, which host only  $\sim 30\%$  of the total baryon mass. Most baryons are in environments with low overdensities, giving rise to very little tSZ signal: more than 60% of baryons are in regions with  $\delta_{gas} < 20$ , which contribute only  $\sim 10\%$  of the total tSZ luminosity. More than two thirds of the diffuse tSZ luminosity (not generated in collapsed structures) is coming from overdense environments with  $\delta_{gas} > 10$  such as filaments or superclusters. The significant amount of baryons present in underdense regions ( $\sim 18\%$  where  $\delta_{gas} < 0$ ) is practically invisible to the tSZ effect ( $\sim 0.5\%$  contribution to tSZ luminosity). While the tSZ will be, at best, sensitive to  $\delta_{gas} > 10$  (i.e. superclusters and filaments), which corresponds to  $\sim 50\%$  of all baryons, X-rays are only sensitive to the core centers of galaxy clusters in our neighborhood which corresponds to

<sup>1</sup> Department of Physics and Astronomy, University of Pennsylvania, Philadelphia, PA 19104, USA; carloshm@astro.upenn.edu; lverde, raulj@physics.upenn.edu

<sup>2</sup> Department of Astrophysical Sciences, Princeton, NJ 08544, USA; htrac@astro.princeton.edu

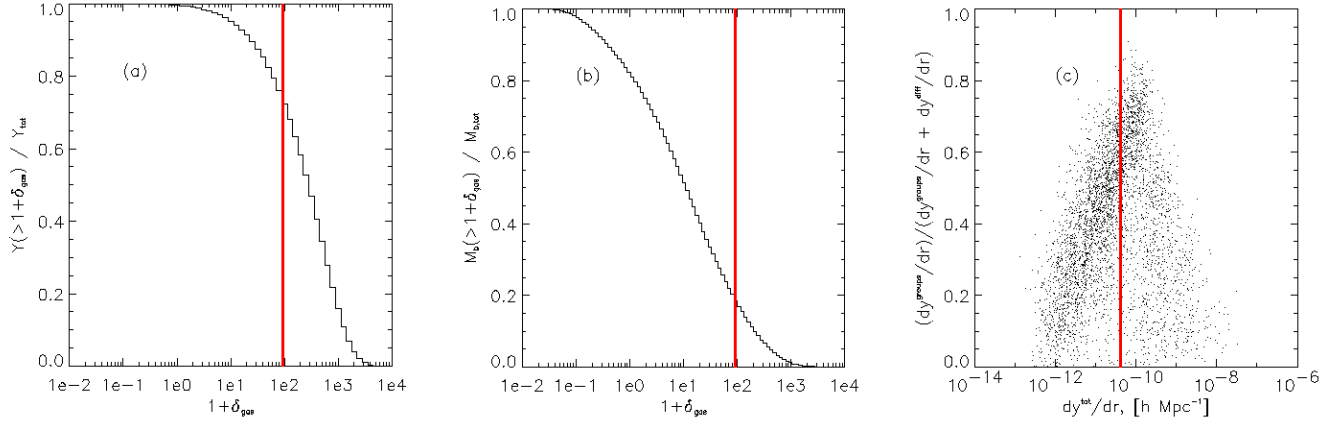


FIG. 1.— (a) Relative contribution to the total tSZ luminosity of regions with gas density contrast bigger than  $\delta_{gas}$ . The vertical solid line indicates the average gas overdensity in haloes. (b) Relative contribution to the total baryon mass of regions with gas density contrast bigger than  $\delta_{gas}$ . The vertical solid line indicates the average gas overdensity in haloes. Note the asymmetry with respect to the previous (left hand side) panel. (c) Ratio of gas pressure produced in galaxy groups (small haloes) over pressure produced by diffuse gas *and* galaxy groups, versus total pressure (including galaxy clusters), averaged on scales of  $12 h^{-1} \text{Mpc}$ . The solid vertical line corresponds to regions with average matter density. In overdense regions, the pressure of haloes always dominates the diffuse pressure.

less than 5% of all baryons, (Fukugita & Peebles 2004).

Because in overdense regions most of the tSZ is generated in haloes, we find a tight correlation between the gas pressure giving rise to the tSZ and the number galaxy density field,  $p_e \propto n_{gal}^{2.2}$ . This allows us to build tSZ templates and to make predictions for the tSZ signal from existing galaxy surveys.

## 2. NUMERICAL SIMULATIONS

We ran a cosmological simulation of a LCDM cosmology ( $\Omega_m = 0.3, \Omega_\Lambda = 0.7, \Omega_b = 0.045, h = 0.7, \sigma_8 = 0.9, n = 1$ ) with a box of  $200 \text{ Mpc}/h$  side,  $1024^3$  hydro grid cells, and  $512^3$  dark matter particles using the TVD+PM code of Trac & Pen (2004). The comoving grid spacing is  $195 \text{ kpc}/h$  and the dark matter particle mass resolution is  $5 \times 10^9 M_\odot/h$ . The Eulerian hydro algorithm computes the spatial and temporal changes in the conserved mass, momentum, and total energy. The thermal energy is calculated by subtracting the kinetic energy from the total energy, while the pressure and temperature are related to the thermal energy by the standard equation of state. The simulation is adiabatic. We recall the definition of the Comptonization parameter ( $y \equiv \int dr \sigma_T n_e (k_B T_e) / (m_e c^2)$ , with  $\sigma_T$  the Thomson cross-section,  $k_B$  the Boltzmann constant and  $m_e, n_e, T_e$  the electron mass, density and temperature, respectively), in order to introduce the derivative  $dy/dr$  as a proxy for electron pressure, ( $dy/dr \propto p_e \propto n_e T_e$ ). Likewise, we define  $Y \equiv \int d^3r dy/dr$ , as a proxy for tSZ luminosity, since both quantities are also proportional. Bound dark matter particles classified as haloes are identified using an ellipsoidal overdensity threshold of 200 times the average density. This defines the halo boundaries which are used to distinguish between tSZ generated in collapsed structures and in the diffuse phase.

## 3. WHERE IS THE TSZ PRODUCED?

We distinguish tSZ luminosity being generated in cells belonging to *clusters of galaxies* ( $M_{cl} \geq 5 \times 10^{13} h^{-1} M_\odot$ ), to *small* haloes (also referred to as *galaxy groups*, and de-

fined as all haloes resolved in the simulation with masses below  $5 \times 10^{13} h^{-1} M_\odot$ ), and to a *diffuse* gaseous phase (defined as all gas cells not belonging to any halo). Given the dark mass particle resolution in our simulation, we choose our mass threshold for the halo definition to be  $\sim 10^{12} h^{-1} M_\odot$ : all haloes below this limit are regarded as diffuse gas, and hence our estimates for the diffuse tSZ contribution should be regarded as optimistic.

Figure (1a) shows the cumulative distribution of the pressure in the box versus gas density contrast. Collapsed structures show a halo-mass-weighted average gas overdensity of  $\sim 93$ , (marked by the vertical solid line). When integrating -i.e., volume weighting- the tSZ luminosity in the three cell subsets defined above (galaxy clusters, small haloes and diffuse gas), we find that  $\sim 70\%$  of total tSZ luminosity is generated in galaxy clusters, and, out of the  $\sim 30\%$  remaining, around one third of it (i.e.,  $\sim 10\%$  of the total) is generated in small haloes. This leaves the diffuse phase a  $\sim 20\%$  contribution, even though it hosts  $\sim 70\%$  of the total baryonic mass. Further, one fourth of this diffuse gas is located in underdense regions, whose tSZ luminosity is negligible ( $< 1\%$ ). This asymmetry of the pressure and baryon mass distributions versus gas overdensity is explicitly shown in Figures (1a,b).

This suggests that the detection, via the tSZ effect, of the diffuse gas will be hampered by the presence of small (and plausibly unresolved) haloes: this is shown in Figure (1c), where the ratio of the gas pressure generated in small haloes over the sum of the contributions from the diffuse gas and small haloes is plotted versus the total gas pressure, (in all cases the pressure is computed in cells of  $12 h^{-1} \text{Mpc}$  side). The vertical line marks the total pressure corresponding to the average galaxy number density. We see that, in slightly overdense regions hosting large pressure (right of the vertical line), the tSZ luminosity outside galaxy clusters is preferentially generated in smaller haloes rather than in diffuse gas, i.e., when searching for the tSZ signature of diffuse gas in overdense regions one must carefully subtract the

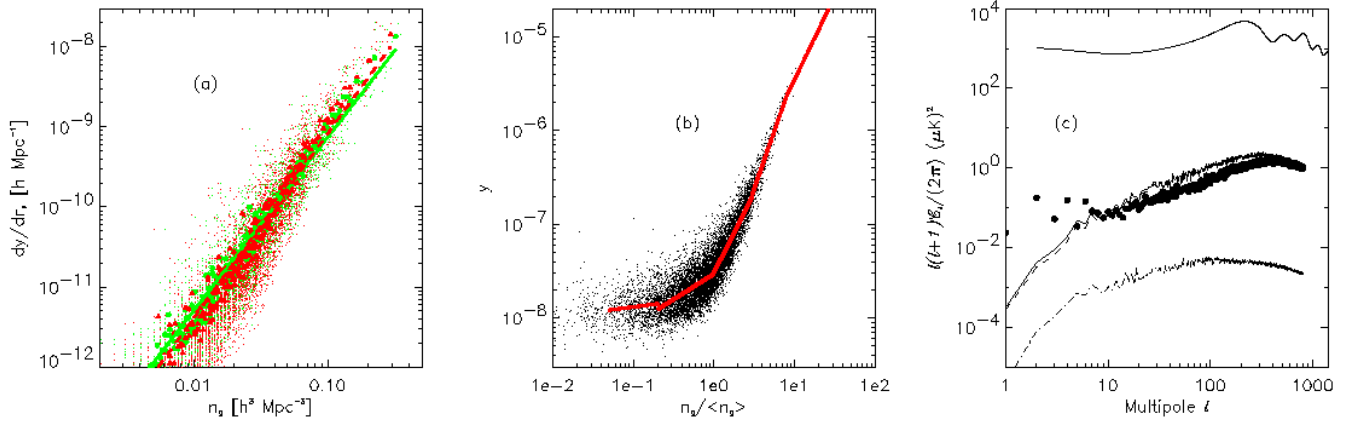


FIG. 2.— (a) Pressure – galaxy number density correlation, according to SSHJ (filled circles and solid line) and K04 (filled triangles, dashed line) prescription to populate haloes with galaxies. (b) Correlation between Comptonization parameter  $y$  and projected galaxy overdensity (K04 prescription) obtained after projecting a simulated sphere of  $300 h^{-1}$  Mpc radius. (c) Rayleigh-Jeans (RJ) expectation for our prediction of the local tSZ power spectrum computed from 2MASS galaxy catalog and the  $y$ -galaxy correlation (filled circles). The tSZ power spectrum (RJ) from our simulated volume is given by the solid line, and decomposed into the halo (dashed line) and diffuse (dot-dashed line) contributions.

contribution from small haloes. Projection effects in future CMB maps will further enhance this contamination. Only when considering the very overdense regions of the universe (far right end of this plot), the relative weight of the diffuse phase takes over, since in such environments there are no small haloes (all haloes are clusters). Note however that the mass threshold for our cluster definition ( $5 \times 10^{13} h^{-1} M_\odot$ ) corresponds to abundant and not-so-tSZ-bright objects, and that these sources may still be responsible for a significant amount of confusion noise.

#### 4. THE PRESSURE - HALO CORRELATION

Since more than 80% of the tSZ luminosity is generated in collapsed structures, there must be a correlation between the gas pressure and the number density of haloes, or the gas pressure and the galaxy number density.

To investigate this correlation, we populate the haloes in the simulation using two different algorithms: the first one (Scoccimarro et al. (2001), hereafter SSHJ) characterizes the halo galaxy population by a binomial distribution, whereas the second (Kravtsov et al. (2004), hereafter K04) uses a Poissonian distribution. As in Smith et al. (2006), both algorithms are normalized to give the same average galaxy number density, ( $\langle n_g \rangle \simeq 3 \times 10^{-2} h^3 \text{Mpc}^{-3}$ ), and this requires slightly different choices for the halo minimum mass hosting a galaxy. As shown in Figure (2a), the correlation found between  $dy/dr$  and galaxy number density (computed in cells of  $12 h^{-1} \text{Mpc}$  side) is very similar in both cases, and well fitted by a power law of index  $n \approx 2.1 - 2.3$  for the SSHJ and K04 methods (filled circles and filled triangles, solid and dashed lines, respectively). The slope obtained in both cases is close to the prediction that a polytropic gas model ( $p \propto \rho^\gamma$ ) provides for a self-gravitating system, ( $\gamma = 2$ ).

As current all sky maps of the local galaxy distribution do not have distance information, we want to investigate the correlation between projected galaxy density and  $y$ . We extend our simulated volume to a box of  $600 h^{-1} \text{Mpc}$  side, exploiting the fact that the simulation

box has periodic boundary conditions. We then place an observer in the center and project on a HEALPix (Górski et al. 2005) map of resolution parameter  $N_{\text{side}} = 512$  a sphere of  $300 h^{-1} \text{Mpc}$  radius. We produce maps of  $y$  and galaxies, smooth them with a Gaussian beam of  $\text{FWHM} = 12.6$  arcmins, and sort the pixels in increasing projected number of galaxies. After binning them in groups of 32 pixels (for display purposes), we obtain a correlation between  $y$  and the projected galaxy overdensity ( $n_g(\hat{n})/\langle n_g \rangle$ ,  $\hat{n}$  denoting a direction on the sky), shown in Figure (2b).

We find that for slight galaxy overdensities (few times the background density), there is a tight correlation between galaxy number density and the Comptonization parameter  $y$ . This suggests using existing galaxy catalogs to predict the degree of Comptonization of the CMB sky. The volume used in our projection is close to that sampled by the Two Micron All Sky Survey (hereafter 2MASS, Jarrett et al. (2003)). We thus use a map of projected galaxies from this survey (constructed as in Hernández-Monteagudo et al. (2004)) to make a prediction of the  $y$  sky. When comparing the galaxy maps from 2MASS and our simulation we find that they both show similar galaxy densities and clustering properties. We approximate the correlation given in Figure (2b) by five power laws (given by the solid lines), and invert the 2MASS-based galaxy catalog into a  $y$  map.

The overall  $y$  normalization is set by imposing that the 256 highest density pixels have a tSZ decrement of  $-73 \pm 17 \mu\text{K}$ , as found at 94 GHz by Hernández-Monteagudo et al. (2004) (all maps have been convolved by the same Gaussian beam). The power spectrum of the resulting  $y$  map (in units of  $[\mu\text{K}]^2$  at Rayleigh-Jeans frequencies) is shown in Figure (2c) by filled circles: its amplitude and shape is very close, at high multipoles, to the power spectrum of the  $y$  map produced from our simulation (solid line). They only differ clearly at large scales ( $\ell < 10$ ), for which the  $y$  power spectrum estimated from 2MASS is higher. This prediction for the local tSZ power spectrum is remark-

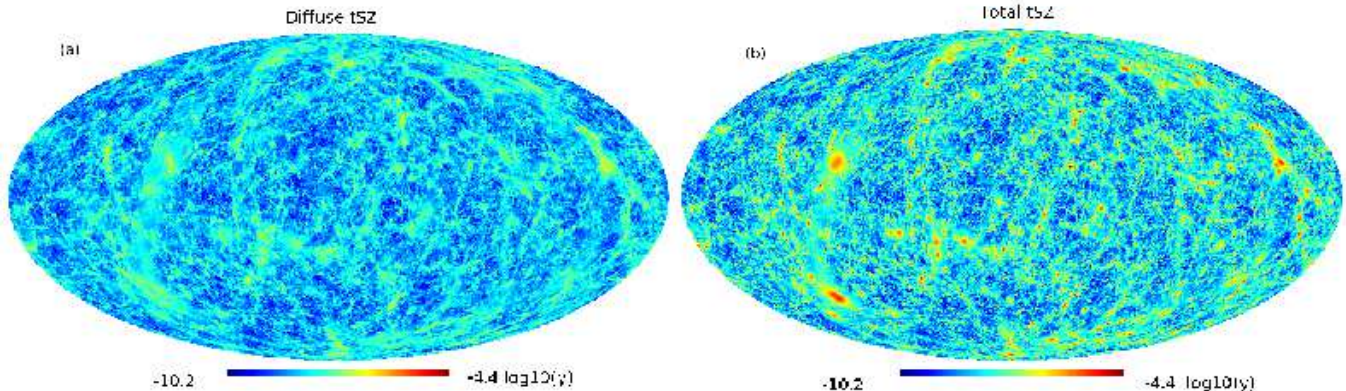


FIG. 3.— (a) All-sky diffuse tSZ contribution in our simulated volume, as opposed to the total tSZ contribution, (panel (b)).

ably close both in shape and amplitude to those obtained by Hansen et al. (2005); Dolag et al. (2005) via a independent approach. Our computation should be a valid prediction for the tSZ power at low  $\ell$ s, but at high  $\ell$ s the neglected high-redshift cluster population will dominate.

#### 5. PROSPECTS FOR DIFFUSE TSZ DETECTION

Since we have separated in our simulation the gas belonging to collapsed haloes from the gas in a diffuse phase, it is possible to compute  $y$  maps and power spectra of the halo and the diffuse components separately. The dot-dashed line at the bottom of Figure (2c) provides the power spectrum of the diffuse gas in our simulation, whereas the dashed line corresponds to the tSZ power spectrum generated by gas located in haloes (note its proximity to the total contribution [solid line]). A map of diffuse tSZ is given in Figure (3a), and comparing to the total tSZ contribution (Figure (3b)). We conclude that most of the diffuse tSZ signal visible on the CMB sky (and more than 90% of the total tSZ luminosity) is generated in overdense regions traced by the clusters and superclusters, (i.e., the diffuse warm gaseous component present in voids leaves negligible tSZ signature). The amplitude of the diffuse phase is at best ten times (a hundred times in  $C_\ell$ 's) smaller than the tSZ signal generated in haloes, *even at large angular scales*. In particular since galaxies trace superclusters and filaments (corresponding to  $\delta_{gas} > 10$ ), the diffuse gas in these regions could be targeted by tSZ

observations with specifications similar to those of e.g. ACT (<http://www.hep.upenn.edu/act/>). These regions contain 50% of the baryons: thus tSZ observations may decrease the ratio of unseen baryons in the local universe from  $\sim 9$  to  $\sim 2$ . In practice, the limiting factor in detecting this signal will be confusion noise from unresolved haloes. Note that the ratio of tSZ luminosities of the collapsed and diffuse baryon components does not equal the ratio of the corresponding tSZ-induced angular power spectra, since the latter quantities depend on the contrast of tSZ sources against the CMB background. This makes the search for the (diffuse) missing baryons even more challenging. The detection of part of the diffuse tSZ may be feasible in nearby superclusters after masking out all compact sources and well characterized nearby galaxy clusters. However, we must conclude that the tSZ, despite of providing a new tool to unveil the presence of unseen warm and hot gas, will still miss a significant fraction of the baryons in the local Universe.

We thank R.E.Smith and R.Sheth for useful discussions. We acknowledge the use of HEALPix (Górski et al. 2005) package, and the Two Micron All Sky Survey. CHM is supported by NASA grants ADP03-0092 and ADP04-0093 and NSF grant PIRE-0507768. RJ is partially supported by NSF grant PIRE-0507768 and by NASA grant NNG05GG01G. LV is supported by NASA grants ADP03-0092 and ADP04-0093.

#### REFERENCES

- Astier, P., et al. 2006, *A&A*, 447, 31  
Atrio-Barandela, F. & Mücke, J. P. 2006, *ApJ*, 643, 1  
Battistelli, E. S., et al. 2006, *ArXiv Astrophysics e-prints*, arXiv:astro-ph/0603702  
Böhringer, H., et al. 2000, *ApJS*, 129, 435  
Cen, R., & Ostriker, J. P. 2005, *ArXiv Astrophysics e-prints*, arXiv:astro-ph/0601008  
Cen, R., & Ostriker, J. P. 1999, *ApJ*, 514, 1  
Cole, S., et al. 2005, *MNRAS*, 362, 505  
Croft, R. A. C., Weinberg, D. H., Katz, N., & Hernquist, L. 1998, *ApJ*, 495, 44  
Dolag, K., Hansen, F. K., Roncarelli, M., & Moscardini, L. 2005, *MNRAS*, 363, 29  
Fukugita, M., & Peebles, P. J. E. 2004, *ApJ*, 616, 643  
Génova-Santos, R., et al. 2005, *MNRAS*, 363, 79  
Górski, K.M., E. Hivon, A.J. Banday, B.D. Wandelt, F.K. Hansen, M. Reinecke, & M. Bartelmann, 2005 *ApJ*, 622, 759  
Hansen, F. K., Branchini, E., Mazzotta, P., Cabella, P., & Dolag, K. 2005, *MNRAS*, 361, 753  
Hernández-Monteagudo, C., Génova-Santos, R., & Atrio-Barandela, F. 2004, *ApJL*, 613, L89  
Jarrett, T. H., Chester, T., Cutri, R., Schneider, S. E., & Huchra, J. P. 2003, *AJ*, 125, 525  
Kravtsov, A. V., Berlind, A. A., Wechsler, R. H., Klypin, A. A., Gottlöber, S., Allgood, B., & Primack, J. R. 2004, *ApJ*, 609, 35  
Kull, A., Böhringer, H. 1999, *A&A*, 341, 23  
McDonald, P., et al. 2005, *ApJ*, 635, 761  
Motl, P. M., Hallman, E. J., Burns, J. O., & Norman, M. L. 2005, *ApJ*, 623, L63  
Nicastrò, F., et al. 2005, *ApJ*, 629, 700  
Nicastrò, F., et al. 2005, *Nature*, 433, 495  
Soccimarro, R., Sheth, R. K., Hui, L., & Jain, B. 2001, *ApJ*, 546, 20  
Sheth, R. K., & Tormen, G. 1999, *Mon. Not. Roy. Astron. Soc.*, 308, 119

- Smith, R. E., Watts, P. I. R., & Sheth, R. K. 2006, MNRAS, 365, 214
- Spergel, D. N., et al. 2003, ApJS, 148, 175
- Spergel, D. N., et al. 2006, ArXiv Astrophysics e-prints, arXiv:astro-ph/0603449
- Sunyaev, R. A., & Zeldovich, Y. B. 1980, ARA&A, 18, 537
- Tegmark, M., et al. 2004, ApJ, 606, 702
- Trac, H., & Pen, U.-L. 2004, New Astronomy, 9, 443
- Zappacosta, L., Mannucci, F., Maiolino, R., Gilli, R., Ferrara, A., Finoguenov, A., Nagar, N. M., & Axon, D. J. 2002, A&A, 394, 7